ACS APPLIED MATERIALS & INTERFACES

Research Article

www.acsami.org

Bis(tri-*n*-hexylsilyl oxide) Silicon Phthalocyanine: A Unique Additive in Ternary Bulk Heterojunction Organic Photovoltaic Devices

Benoît H. Lessard,[†] Jeremy D. Dang,[†] Trevor M. Grant,[†] Dong Gao,[‡] Dwight S. Seferos,[†,‡] and Timothy P. Bender*[,†,‡,§]

[†]Department of Chemical Engineering and Applied Chemistry, University of Toronto, 200 College Street, Toronto, Ontario M5S 3E5, Canada

[‡]Department of Chemistry, University of Toronto, 80 St. George Street, Toronto, Ontario M5S 3H6, Canada

[§]Department of Materials Science and Engineering, University of Toronto, 184 College Street, Toronto, Ontario M5S 3E4, Canada

Supporting Information

ABSTRACT: Previous studies have shown that the use of bis(tri-*n*-hexylsilyl oxide) silicon phthalocyanine ($(3HS)_2$-SiPc) as an additive in a P3HT:$PC_{61}BM$ cascade ternary bulk heterojunction organic photovoltaic (BHJ OPV) device results in an increase in the short circuit current (J_{SC}) and efficiency (η_{eff}) of up to 25% and 20%, respectively. The previous studies have attributed the increase in performance to the presence of $(3HS)_2$-SiPc at the BHJ interface. In this study, we explored the molecular characteristics of $(3HS)_2$-SiPc which makes it so effective in increasing the OPV device J_{SC} and η_{eff}. Initially, we synthesized phthalocyanine-based additives using different core elements such as germanium and boron instead of silicon, each having similar frontier orbital energies compared to $(3HS)_2$-SiPc and tested their effect on BHJ OPV device performance. We observed that addition of bis(tri-*n*-hexylsilyl oxide) germanium phthalocyanine ($(3HS)_2$-GePc) or tri-*n*-hexylsilyl oxide boron subphthalocyanine (3HS-BsubPc) resulted in a nonstatistically significant increase in J_{SC} and η_{eff}. Secondly, we kept the silicon phthalocyanine core and substituted the tri-*n*-hexylsilyl solubilizing groups with pentadecyl phenoxy groups and tested the resulting dye in a BHJ OPV. While an increase in J_{SC} and η_{eff} was observed at low $(PDP)_2$-SiPc loadings, the increase was not as significant as $(3HS)_2$-SiPc; therefore, $(3HS)_2$-SiPc is a unique additive. During our study, we observed that $(3HS)_2$-SiPc had an extraordinary tendency to crystallize compared to the other compounds in this study and our general experience. On the basis of this observation, we have offered a hypothesis that when $(3HS)_2$-SiPc migrates to the P3HT:$PC_{61}BM$ interface the reason for its unique performance is not solely due to its frontier orbital energies but also might be due to a high driving force for crystallization.

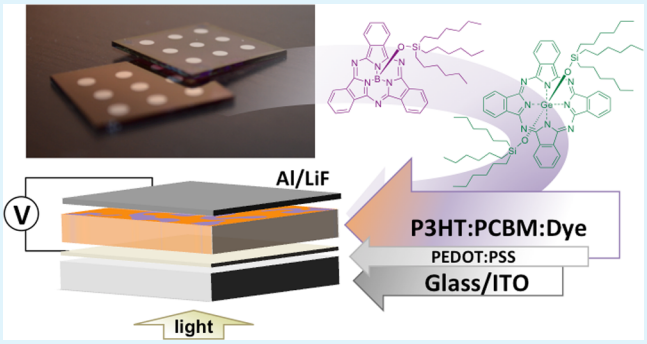

KEYWORDS: *boron, germanium, silicon, phthalocyanine, ternary, cascade, bulk, heterojunction, solar, cell, photovoltaic, P3HT, $PC_{61}BM$*

INTRODUCTION

Over the past decade, the interest in organic photovoltaic devices (OPVs) has grown exponentially.[1−4] While promising results have been reported for both bilayer and planar heterojunction OPV device structures,[5−8] the majority of the literature is focused on the fabrication of bulk heterojunction (BHJ) OPVs that utilize the blending of donor−acceptor polymers and/or small molecules which mutually phase separate when deposited as a single functional layer. Recently, OPVs based on BHJ configurations have been reported to have power conversion efficiencies (η_{eff}) approaching 9% using a variety of unique synthetic polymers.[9−13]

P3HT and $PC_{61}BM$ (poly(3-hexylthiophene):phenyl-C_{61}-butyric acid methyl ester, Figure 1) are arguably the most studied donor−acceptor pair of materials used as an active layer in a BHJ OPV, with countless publications showing these devices having η_{eff} ranging between 2% and 5%.[14] Several factors such as compound purity, annealing temperature and time, the use of a low boiling solvent and additives, and the overall ratio of P3HT to $PC_{61}BM$ have all been identified as contributors to this variation in efficiency.[14,15] It is accepted that the energy levels associated with P3HT and $PC_{61}BM$ are not ideal and that increased efficiency could or can result from modifying the energy levels of the frontier molecular orbitals of P3HT or $PC_{61}BM$.[16,17]

In place of altering the energy levels of the frontier orbitals of the main active materials, another method which has been shown to increase P3HT:$PC_{61}BM$ BHJ OPV device efficiency

Received: May 16, 2014
Accepted: August 8, 2014
Published: August 8, 2014

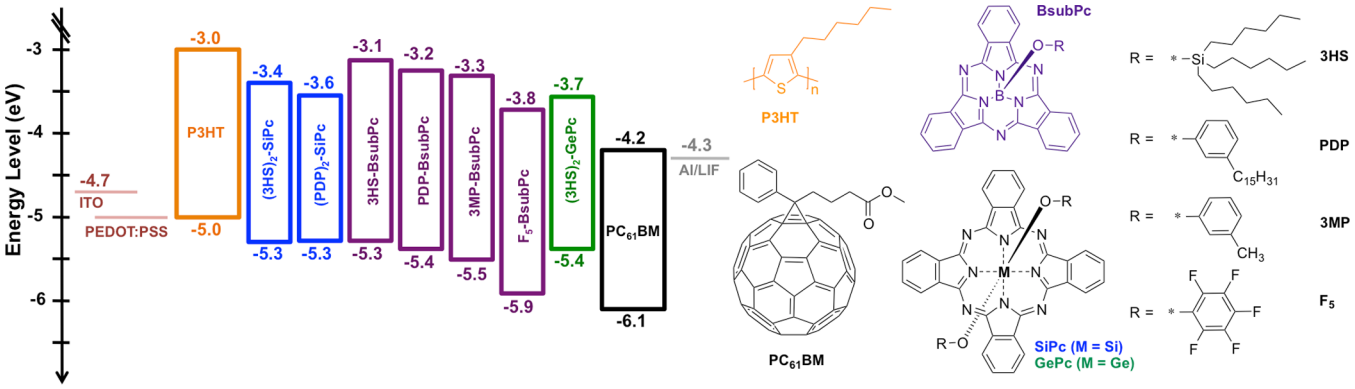

Figure 1. Energy level diagram and chemical structure of poly(3-hexylthiophene) (P3HT), bis(tri-*n*-hexylsilyl oxide) silicon phthalocyanine ($(3HS)_2$-SiPc), bis(3-pentadecylphenoxy)-silicon phthalocyanine ($(PDP)_2$-SiPc), tri-*n*-hexylsilyl oxide boron subphthalocyanine (3HS-BsubPc), 3-pentadecylphenoxy boron subphthalocyanine (PDP-BsubPc). 3-methylphenoxy boron subphthalocyanine (3MP-BsubPc), pentafluorophenoxy boron subphthalocyanine (F_5-BsubPc), bis(tri-*n*-hexylsilyl oxide) germanium phthalocyanine ($(3HS)_2$-GePc), and phenyl-C_{61}-butyric acid methyl ester ($PC_{61}BM$). The energy levels of the HOMOs and LUMOs were either taken from the literature or derived from electrochemistry (Table 2).

Table 1. P3HT:$PC_{61}BM$:*X* (where *X* is Tertiary Additive) Ratios for BHJ OPV Device Fabrication and the Resulting Device Characterization[a]

P3HT:$PC_{61}BM$:*X*[b] (mass ratio)	wt %[c]	*X*	J_{SC} [mA cm^{-2}]	V_{OC} [V]	FF [%]	η_{eff} [%]
1:0.8:0			8.48 ± 0.42	0.57 ± 0.01	0.56 ± 0.03	2.74 ± 0.22
1:0.8:0.2	10.6	$(3HS)_2$-SiPc	10.58 ± 0.27	0.59 ± 0.02	0.51 ± 0.01	3.17 ± 0.08
1:0.8:0.1	5.3	$(3HS)_2$-SiPc	9.10 ± 0.82	0.56 ± 0.02	0.52 ± 0.02	2.68 ± 0.38
1:0.8:0.07	3.7	$(3HS)_2$-SiPc	9.84 ± 0.15	0.57 ± 0.005	0.59 ± 0.01	3.29 ± 0.09
1:0.8:0.1	5.3	$(3HS)_2$-GePc	0.35 ± 0.03	0.12 ± 0.01	0.24 ± 0.01	0.012 ± 0.002
1:0.8:0.07	3.7	$(3HS)_2$-GePc	0.62 ± 0.01	0.16 ± 0.01	0.24 ± 0.01	0.023 ± 0.002
1:0.8:0.2	10.6	3HS-BsubPc	8.75 ± 0.28	0.55 ± 0.005	0.44 ± 0.04	2.10 ± 0.18
1:0.8:0.1	5.3	3HS-BsubPc	8.69 ± 0.43	0.56 ± 0.01	0.57 ± 0.01	2.76 ± 0.15
1:0.8:0.07	3.7	3HS-BsubPc	9.20 ± 0.32	0.55 ± 0.005	0.58 ± 0.01	2.92 ± 0.07
1:0.8:0.2	10.6	PDP-BsubPc	7.69 ± 0.33	0.57 ± 0.005	0.52 ± 0.18	2.27 ± 0.18
1:0.8:0.1	5.3	PDP-BsubPc	7.77 ± 0.23	0.57 ± 0.005	0.51 ± 0.04	2.26 ± 0.22
1:0.8:0.07	3.7	PDP-BsubPc	7.90 ± 0.27	0.55 ± 0.005	0.61 ± 0.01	2.63 ± 0.11
1:0.8:0.2	10.6	3MP-BsubPc	6.99 ± 0.51	0.51 ± 0.03	0.37 ± 0.01	1.30 ± 0.16
1:0.8:0.1	5.3	3MP-BsubPc	7.03 ± 0.62	0.57 ± 0.005	0.47 ± 0.01	1.90 ± 0.15
1:0.8:0.1	5.3	F_5−BsubPc	6.68 ± 0.78	0.50 ± 0.01	0.33 ± 0.02	1.08 ± 0.06
1:0.8:0.1:0.1[d]	5.3/5.3	F_5/3MP-BsubPc	6.93 ± 0.31	0.48 ± 0.02	0.29 ± 0.005	0.96 ± 0.09
1:0.8:0.05:0.05[d]	2.7/2.7	F_5/3MP-BsubPc	8.27 ± 0.40	0.56 ± 0.01	0.37 ± 0.01	1.68 ± 0.14
1:0.8:0.2	10.6	$(PDP)_2$-SiPc	8.94 ± 0.09	0.58 ± 0.01	0.46 ± 0.01	2.34 ± 0.03
1:0.8:0.1	5.3	$(PDP)_2$-SiPc	7.94 ± 0.20	0.58 ± 0.01	0.53 ± 0.01	2.44 ± 0.08
1:0.8:0.07	3.7	$(PDP)_2$-SiPc	9.49 ± 0.20	0.59 ± 0.01	0.54 ± 0.01	3.02 ± 0.08

[a]In all cases, the values were averaged with a minimum of 4−5 devices. In the case of Exp. A, B, and C, the values were averaged over a minimum of 2−3 devices with 4−5 pixels on each device fabricated over the span of 8−12 weeks in the same apparatus. The values were obtained under AM1.5G irradiation at 100 mW cm^{-2}. [b]Mass ratio used to fabricate the active layer of the bulk heterojunction organic photovoltaic (BHJ-OPV) devices, where P3HT represents poly(3-hexylthiophene), $PC_{61}BM$ represents phenyl-C_{61}-butyric acid methyl ester, $(3HS)_2$-SiPc represents bis(tri-*n*-hexylsilyl oxide) silicon phthalocyanine, 3HS-BsubPc represents tri-*n*-hexylsilyl oxide boron subphtahlocyanine, $(3HS)_2$-GePc represents bis(tri-*n*-hexylsilyl oxide) germanium phthalocyanine, and $(PDP)_2$-SiPc represents bis(3-pentadecyl phenoxy)-silicon phthalocyanine. [c]wt % is the weight percent of the additive relative to the P3HT:$PC_{61}BM$. [d]Quarternary BHJ OPV devices: P3HT:$PC_{61}BM$:3MP-BsubPc:F_5-BsubPc.

is to incorporate a third component, either a small molecule or polymer, to act as a second donor or acceptor. This configuration is referred to as a cascade BHJ whereby the increase in device η_{eff} is achieved by increasing the light absorption, exciton dissociation, or even hole or electron transfer between the P3HT and $PC_{61}BM$ or $PC_{71}BM$ domains.[18−23] For example, Chen et al. utilized an ambipolar poly[2,3-bis(thiophen-2-yl)-acrylonitrile-9,9′-dioctyl-fluorene] polymer as an additive in a P3HT:$PC_{61}BM$ cascade BHJ OPV device.[24] The authors noted up to a 30% increase in η_{eff} when adding as little as ∼2.5 wt % of the polymer with respect to P3HT:$PC_{61}BM$.[24]

Recently, Honda et al. explored the use of metal-containing phthalocyanines for the formation of a P3HT:$PC_{61}BM$ cascade BHJ.[25,26] An increase of up to 20% in η_{eff} was noted when bis(tri-*n*-hexylsilyl oxide) silicon phthalocyanine ($(3HS)_2$-SiPc, Figure 1) was added to a P3HT:$PC_{61}BM$ BHJ OPV device.[25] The authors further studied this system and determined that $(3HS)_2$-SiPc was present mostly at the P3HT:$PC_{61}BM$ interface[27] and that the efficiency increase came from the increased light absorption due to SiPc chromophore (peak at ≈700 nm) as well as the more efficient electron transfer from P3HT through $(3HS)_2$-SiPc to $PC_{61}BM$ compared to the direct

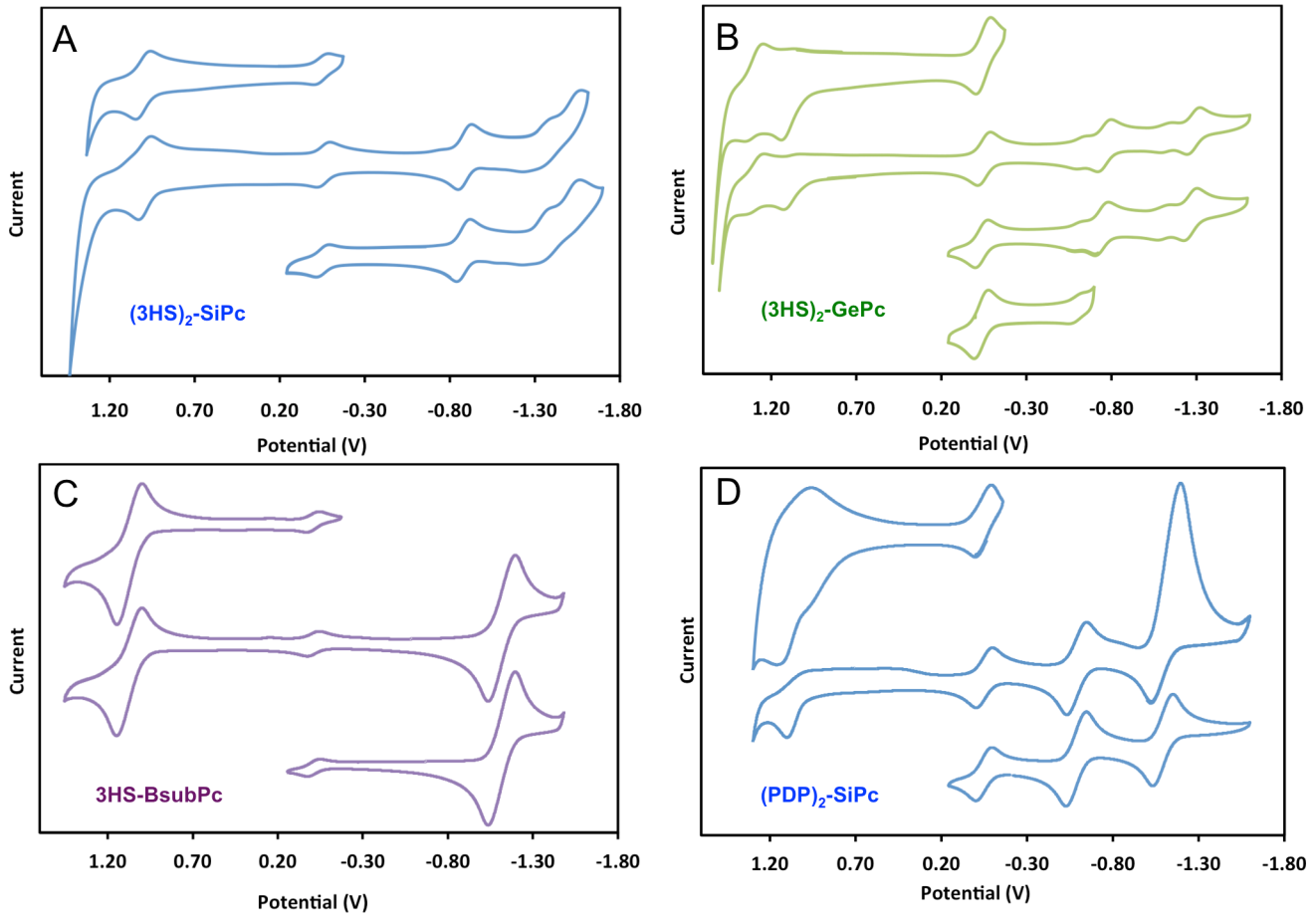

Figure 2. Electrochemical spectra for (A) bis(tri-*n*-hexylsilyl oxide) silicon phthalocyanine ($(3HS)_2$-SiPc), (B) bis(tri-*n*-hexylsilyl oxide) germanium phthalocyanine ($(3HS)_2$-GePc), (C) tri-*n*-hexylsilyl oxide boron subphthalocyanine (3HS-BsubPc), and (D) bis(3-pentadecylphenoxy)-silicon phthalocyanine ($(PDP)_2$-SiPc).

transfer from P3HT to $PC_{61}BM$ without $(3HS)_2$-SiPc present.[28]

Lim et al. recently reported the addition of a bis(tri-*n*-hexylsilyl oxide) silicon naphthalocyanine ($(3HS)_2$-SiNc) into a P3HT:$PC_{61}BM$ BHJ OPV.[29] In one instance, the SiNc was *tert*-butylated around the periphery and in another it was not. At high dye loadings when no *tert*-butyl groups were present, the P3HT:$PC_{61}BM$ morphology was disrupted resulting in a third highly ordered phase and a drop in device characteristics. However, the authors found that, with the addition of the *tert*-butyl groups on the dye, a much higher loading of the dye was possible without a significant change in morphology. Detailed analysis also showed that the SiNc derivatives were present at the interface and that non-*tert*-butylated SiNc had a tendency to form a distinct crystalline third phase at certain loadings.[29]

Coincident with the study of Lim et al.,[29] we were interested in determining if other closely related phthalocyanine compounds could show similar or even better improvements in performance when applied in a P3HT:$PC_{61}BM$ cascade BHJ and compared against $(3HS)_2$-SiPc. In other words, we wanted to understand if $(3HS)_2$-SiPc is unique or whether other structurally and chemically related phthalocyanine dyes could function in the same manner. In this paper, we summarize our exploration of variants of $(3HS)_2$-SiPc and their application in P3HT:$PC_{61}BM$ cascade BHJ OPV devices. Specifically, we have synthesized boron and germanium variants as well as variants of $(3HS)_2$-SiPc and incorporate each into BHJ OPV devices at varying concentrations.

RESULTS AND DISCUSSION

Baseline P3HT:$PC_{61}BM$ BHJ OPV Devices. A series of baseline BHJ OPV devices using the structure ITO/PEDOT:PSS/Active Layer/LiF/Al, where the active layer was a 1.0:0.8 mixture of P3HT:$PC_{61}BM$, was repeatedly fabricated throughout the entire study and constantly analyzed and compared (see Experimental Section for procedure). The resulting BHJ OPV devices were determined to have short circuit current (J_{SC}) = 8.15 ± 0.78 mA·cm^{-2}, V_{OC} = 0.62 ± 0.02 V, FF = 0.55 ± 0.03, and η_{eff} = 2.75 ± 0.21 (averaged over at least 40 devices), which is within the average reported for such devices (Table 1).[14] A representative current versus voltage (IV) curve with error bars and external quantum efficiency (EQE) plot for an average P3HT:$PC_{61}BM$ device are shown in Figure S1, Supporting Information.

P3HT:$PC_{61}BM$ Cascade BHJ OPVs Using $(3HS)_2$-SiPc. As mentioned above, Honda et al. found that the addition of roughly 5 wt % $(3HS)_2$-SiPc increased the generated current as well as the η_{eff} of a P3HT:$PC_{61}BM$ BHJ OPV device.[25,26] The authors also thoroughly studied why and how $(3HS)_2$-SiPc functions in this manner. For example, spectroscopic analysis showed that $(3HS)_2$-SiPc enables more efficient charge transfer from the P3HT to the $PC_{61}BM$ layer.[27,28] AFM and contact

Table 2. Characterization of $(3HS)_2$-SiPc, 3HS-BsubPc, $(3HS)_2$-GePc, and $(PDP)_2$-SiPc

sample	$E_{Red,1/2}$ (V)	$E_{OX,1/2}$ (V)	E_{HOMO} [a] (eV)	E_{LUMO} [b] (eV)	λ_{MAX} [c] (nm)	$E_{Gap,Opt}$ [d] (eV)
$(3HS)_2$-SiPc	−0.85	1.04	−5.31	−3.42/−3.49	663/669	1.82
3HS-BsubPc	−1.12	1.07	−5.34	−3.15/−3.27	571/561	2.07
$(3HS)_2$-GePc	−0.59, −0.72, −1.10, −1.25	1.11, 1.34	−5.38	−3.68/−3.58	674/678	1.80
$(PDP)_2$-SiPc	−0.65, −1.17	0.98	−5.25	−3.62/−3.47	681/765	1.78

[a] $E_{HOMO} = -(4.27 + E_{OX,1/2})$ eV (scaled to an internal standard of decamethylferrocene[50−52]). [b] $E_{LUMO,Electro}/E_{LUMO,Opt}$ where $E_{LUMO,Electro} = -(4.27 + E_{Red,1/2})$ and $E_{LUMO,Opt} = E_{Gap,Opt} - E_{HOMO}$. [c] Maximum absorbance, λ_{MAX}, of respective compounds where $\lambda_{MAX,solution}/\lambda_{MAX,film}$. [d] $E_{Gap,Opt}$ determined from the onset of the solution absorbance spectra.

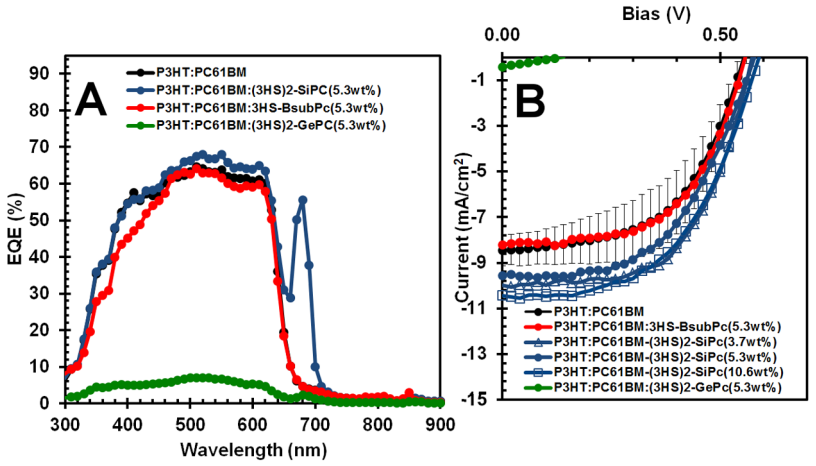

Figure 3. Characteristic (A) external quantum efficiency (EQE) and (B) IV curves for the P3HT:PC_{61}BM (1.0:0.8, mass ratio) and P3HT:PC_{61}BM:*X* (1.0:0.8:*Y*), where *X* = bis(tri-*n*-hexylsilyl oxide) silicon phthalocyanine ($(3HS)_2$-SiPc, 1), tri-*n*-hexylsilyl oxide boron subphtahlocyanine (3HS-BsubPc), and bis(tri-*n*-hexylsilyl oxide) germanium phthalocyanine ($(3HS)_2$-GePc) and where *Y* = 0.2 (10.6 wt %, open squares), 0.1 (5.3 wt %, filled circles), or 0.07 (3.7 wt %, open triangles). Standard P3HT:PC_{61}BM BHJ solar device data (no tertiary additive, black) is shown with error bars to illustrate the space occupied by standard devices.

angle studies using roughly 5 wt % $(3HS)_2$-SiPc determined that 40% of the SiPc molecules are located at the interface.[25]

It is important to note that Honda et al.[25,26] obtained their $(3HS)_2$-SiPc from a "commercial source" and that $(3HS)_2$-SiPc is no longer available in North America from the "commercial source". Therefore, we began our study by synthesizing $(3HS)_2$-SiPc in our laboratory by modifying a patented procedure.[30] We obtained $(3HS)_2$-SiPc in high yields and higher purity than the "commercial source" which was specified at ">85% dye content". See the Experimental Section for details on the synthesis and the Supporting Information for all respective analytics.

Our in house $(3HS)_2$-SiPc was then evaluated as an additive in P3HT:PC_{61}BM BHJ OPV devices with identical device structure to our baseline P3HT:PC_{61}BM OPVs outlined above and using $(3HS)_2$-SiPc loadings similar to those reported by Honda et al.[25,26] The characteristic IV curves and external quantum efficiency (EQE) plots are illustrated in Figure S1, Supporting Information, and the statistics of all the replicates can be found in Table 1. In line with the results of Honda et al.,[25,26] a peak at ≈700 nm due to the SiPc chromophore in the EQE, an increase in J_{SC} of 7−25%, and an increase in η_{eff} of 15−20% were all observed (Figure S1, Supporting Information, Table 1). When adding as much as 10 wt % $(3HS)_2$-SiPc, a decrease in FF was observed, which resulted in a slight decrease in η_{eff} (Figure S1, Supporting Information, Table 1), all consistent with the reports of Honda et al.[25,26] They explained this observation by stating that the incorporation of a larger quantity of dye disrupts the morphology already dictated by the P3HT:PC_{61}BM BHJ resulting in a separate ternary phase for the dye instead of this dye being predominantly present at the interface.[25,26] Given our verification of the results of Honda et al.,[25,26] we can assume that all their other observations and conclusions are valid and replication of their detailed studies is not required by our group for this study.

P3HT:PC_{61}BM Cascade OPVs Using Phthalocyanine Variants. After reproducing the findings by Honda et al.,[25,26] we followed a similar synthetic route to that of $(3HS)_2$-SiPc and synthesized bis(tri-*n*-hexylsilyl oxide) germanium phthalocyanine ($(3HS)_2$-GePc, Figure 1). UV−vis absorbance spectroscopy and electrochemical analysis were performed on both $(3HS)_2$-SiPc and $(3HS)_2$-GePc. Their respective cyclic voltammograms are illustrated in Figure 2A,B, and their calculated highest occupied molecular orbital (HOMO) and lowest unoccupied molecular orbital (LUMO) energy levels along with the absorption maxima are summarized in Figure 1 and Table 2. Interestingly, double reversible oxidation and reduction peaks are observed for $(3HS)_2$-GePc, a finding not observed for $(3HS)_2$-SiPc, which is presumably due to the unique Si−O−Ge−O−Si sequence in $(3HS)_2$-GePc (Figure 1). Apart from the double reversible oxidation and reduction peaks not seen for $(3HS)_2$-SiPc, the estimated HOMO and LUMO energy levels for $(3HS)_2$-GePc appear to be similar to those of $(3HS)_2$-SiPc (Table 2). However, when we introduced $(3HS)_2$-GePc into identical P3HT:PC_{61}BM BHJ OPV devices, the opposite effect was observed to what was found for $(3HS)_2$-SiPc. As little as 3.7 wt % $(3HS)_2$-GePc resulted in a significant decrease in EQE across the spectrum as well as a very large decrease in cell performance characteristics (FF, J_{SC}, and η_{eff}, Figure 3, Table 1). Little literature is available on the electronic

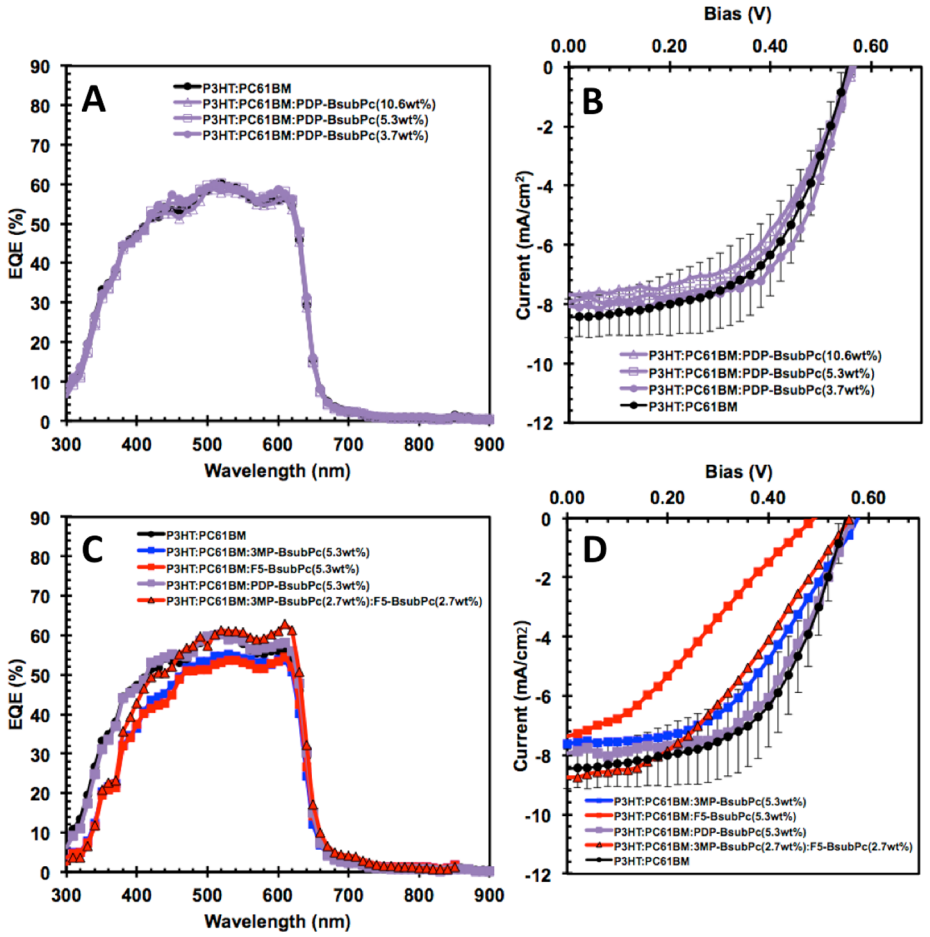

Figure 4. Characteristic (A) external quantum efficiency (EQE) versus wavelength and (B) current versus voltage (IV) plots for P3HT:PC_{61}BM:PDP-BsubPc (1:0.8:*X*, where *X* = 0.2 (10.6 wt %), 0.1 (5.3 wt %), and 0.07 (3.7 wt %)) and as active layer in a BHJ OPV device. Characteristic (C) EQE versus wavelength and (D) IV plots for P3HT:PC_{61}BM:*X* (where *X* = 5.3 wt % addition of 3MP-BsubPc, PDP-BsubPc, or F5-BsubPc or both 2.7 wt % of 3MP-BsubPc and 2.7 wt % of F5-BsubPc) as active layer in BHJ OPV devices. P3HT:PC_{61}BM is the pristine, standard BHJ OPV device (no tertiary additive) with error bars which arise from the standard deviation of all P3HT:PC_{61}BM pristine BHJ OPV devices.

properties of GePcs in general and what is available is significantly out of date.[31,32] We are confident on the analytical purity of $(3HS)_2$-GePc. We are therefore left without an explanation for the significantly detrimental effects of adding $(3HS)_2$-GePc to a P3HT:PC_{61}BM OPV.

Boron subphthalocyanines (BsubPcs) are a class of phthalocyanines that have a unique bowl-shaped heterocyclic structure made out of 3 isoindoline groups as compared to the planar structure of normal phthalocyanines and the presence of 4 isoindoline repeating units in their heterocyclic structure. Recently, BsubPcs have attracted interest as functional components in various organic electronic devices such as organic light emitting diodes (OLEDs),[33,34] OPVs,[8,35−40] and organic thin film transistors (OTFTs).[41,42] The majority of literature examples of BsubPc-based OPV have been limited to the use of chloro-BsubPc (Cl-BsubPc)[33,38,39] which is sparingly soluble and therefore is incorporated into OPV devices by vapor deposition[33,38,39] as opposed to solution processing. While uncommon, a few examples of solution deposition of these BsubPc molecules can be found in the literature. For example, Frechet and co-workers fabricated a series of bilayer OPVs by spin coating a soluble 2-allylphenoxy-BsubPc followed by vapor deposition of C_{60}.[36,37]

To the best of our knowledge, BsubPcs have never been incorporated into BHJ devices. Therefore, we synthesized the analogous BsubPc to $(3HS)_2$-SiPc, tri-*n*-hexylsilyl oxide boron subphthalocyanine (3HS-BsubPc, Figure 1, see Experimental Section and Supporting Information for complete synthesis and characterization). We found it to be exceptionally soluble in common organic solvents. Optical and electrochemical characterization of 3HS-BsubPc were performed, and the results are outlined and tabulated in Figures 1 and 2 and Table 2. On the basis of the measured CV behavior and the calculated HOMO and LUMO energy levels, that are similar to $(3HS)_2$-SiPc, 3HS-BsubPc should result in a cascade BHJ when mixed with P3HT and PC_{61}BM (Figure 1); hence, we introduced 3HS-BsubPc into the identical P3HT:PC_{61}BM BHJ OPV devices as outlined above. The corresponding EQE spectra and IV curve are illustrated in Figure 3. Unlike $(3HS)_2$-SiPc, the absorbance of the 3HS-BsubPc chromophore is at ≈545 nm, and therefore, any photocharge generation from 3HS-BsubPc at low loadings is indistinguishable from charge generated by the combination of P3HT and PC_{61}BM (Figure 3A). Photogeneration from the BsubPc chromophore was observed at increased loadings or when removing PC_{61}BM from the mixture and making a device with just another BsubPc derivative and P3HT (Figure S13, see Supporting Information

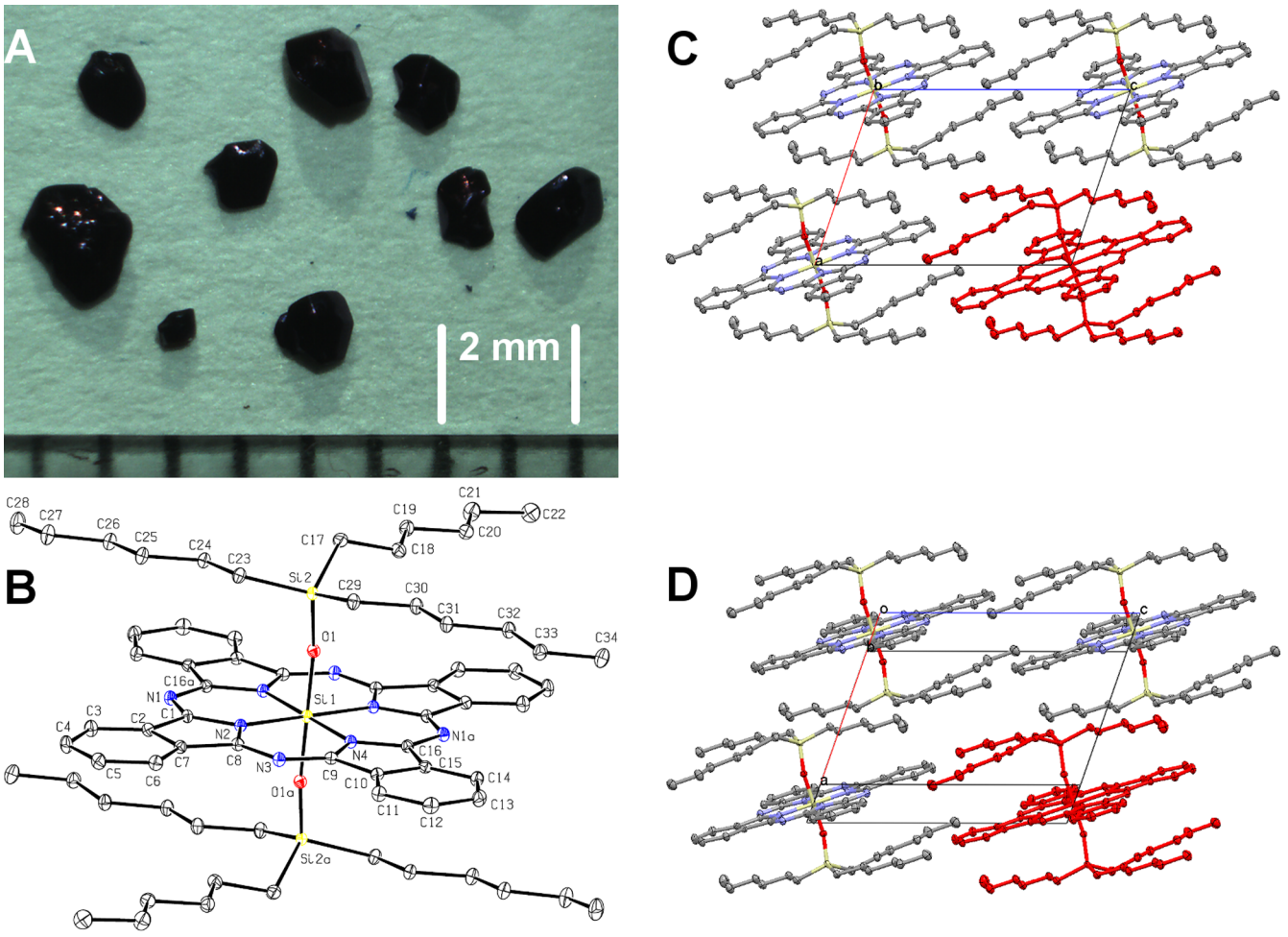

Figure 5. (A) Microscope picture of crystals of $(3HS)_2$-SiPc. (B) Ellipsoid plot (50% probability) showing the structure and atom number scheme of $(3HS)_2$-SiPc (CCDC deposition number: 988974). (C) and (D) are the crystal structure arrangement of multiple $(PDP)_2$-SiPc molecules. In (C) and (D), a single molecule is colored red for clarity. In all cases, hydrogens are omitted for clarity. The unit cell is shown in (B) and (C).

for further discussion). That being said, the addition of 3HS-BsubPc at three different mass loadings did not result in a statistical difference in the measured J_{SC} or V_{OC} of the BHJ OPV devices (Figure 3B, Table 1). The lack of increase in J_{SC} with the addition of 3HS-BsubPc indicates that there is no significant cascade effect between the P3HT and $PC_{61}BM$ via the intermediacy of 3HS-BsubPc despite favorable alignment of the frontier orbitals. On the basis of this, we could presume that a significant portion of 3HS-BsubPc molecules is solubilized in either the P3HT or $PC_{61}BM$ phase rather than being present at the P3HT:$PC_{61}BM$ interface thereby not facilitating the desired electron transfer effect.

We then explored alternative BsubPc derivatives. Our group has several BsubPc variants on hand including 3-pentadecyl-phenoxy-BsubPc[43] (PDP-BsubPc, Figure 1), 3-methyl-phenoxy-BsubPc[44] (3MP-BsubPc, Figure 1), and pentafluoro-phenoxy-BsubPc[8,34] (F_5-BsubPc, Figure 1). These three BsubPcs have similar energy levels to that of 3HS-BsubPc and therefore meet the base energetic criteria to facilitate a cascade electron transfer from P3HT to $PC_{61}BM$ (Figure 1). Each has either similar or differing physical properties than 3HS-BsubPc. For instance, PDP-BsubPc is also highly soluble and the pentadecyl phenoxy fragment has a similar carbon number to the tri-*n*-hexylsilyl fragment. 3MP-BsubPc is an anomalously soluble and crystalline version of BsubPc with a low carbon number for its phenoxy fragment.[44] Finally, F_5-BsubPc is also both relatively soluble and crystalline but has HOMO and LUMO energy levels distinctly different from other BsubPcs[34] (Figure 1). We evaluated each as an additive in ternary BHJ OPV devices, and the resulting characteristics are illustrated in Figure 4 and tabulated in Table 1 (including statistics on the replicates).

Beginning with PDP-BsubPc, the characteristic external quantum efficiency (EQE) and IV curve plots for the P3HT:$PC_{61}BM$:PDP-BsubPc ternary BHJ OPV device are illustrated in Figure 4A,B, respectively. When adding 3.7 wt % PDP-BsubPc, we observe a statistically insignificant increase in J_{SC} and no change in V_{OC} but a statistically significant improvement in FF (56% to 61%) compared to the baseline devices. Increasing the amount of PDP-BsubPc resulted in a statistically significant decrease in device characteristics (Figure 4B, Table 1).

The addition of 3MP-BsubPc or F_5-BsubPc resulted in negligible increases in J_{SC} and a significant decrease in V_{OC} and FF (Figure 4C, Table 1). Figure 4C,D illustrates the comparison between the addition of 5.3 wt % 3MP-BsubPc, F_5-BsubPc, and PDP-BsubPc to the baseline device and the use of a mixture of 2.7 wt % 3MP-BsubPc and 2.7 wt % F_5-BsubPc in the same baseline device. The combination of 3MP-BsubPc and F_5-BsubPc was tested with the idea that the energetic

dx.doi.org/10.1021/am503038t | ACS Appl. Mater. Interfaces 2014, 6, 15040−15051

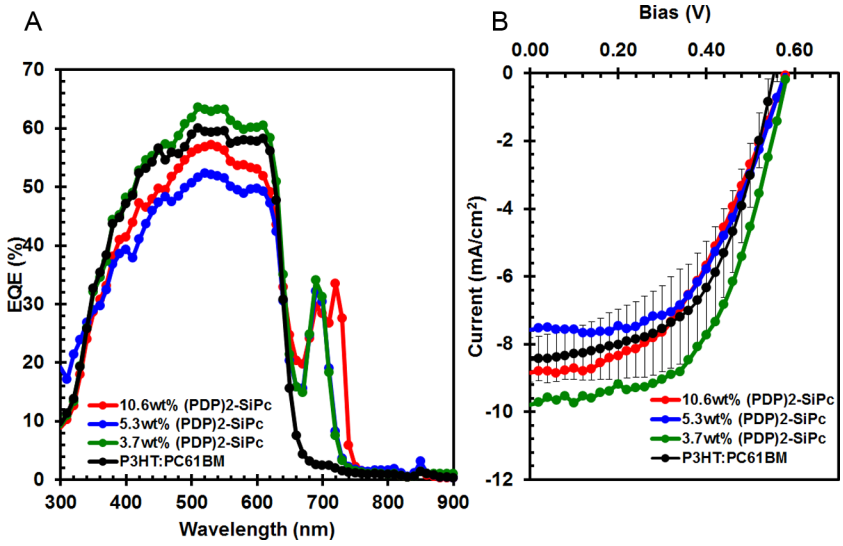

Figure 6. Characteristic (A) external quantum efficiency (EQE) versus wavelength and (B) current versus voltage (IV) plots for P3HT:$PC_{61}BM$:$(PDP)_2$-SiPc (1:0.8:*X*, where *X* = 0.2 (10.6 wt %), 0.1 (5.3 wt %), and 0.07 (3.7 wt %)) and as active layer in a BHJ OPV device. P3HT:$PC_{61}BM$ is the pristine, standard BHJ OPV device (no tertiary additive) with error bars which arise from the standard deviation of all P3HT:$PC_{61}BM$ pristine BHJ OPV devices as outlined in the Baseline P3HT:PC61BM BHJ OPV Devices section.

differences between P3HT, $PC_{61}BM$, 3MP-BsubPc, and F_5-BsubPc would create a favorable cascade of electron transfer effect with lower energetic barrier and an increase in extracted current. Indeed, using the combination of 2.7 wt % 3MP-BsubPc and 2.7 wt % F_5-BsubPc, the P3HT:$PC_{61}BM$ BHJ OPV ternary device did exhibit a statistically significant increase in J_{SC} compared to the use of 5.3 wt % 3MP-BsubPc or 5.3 wt % F_5-BsubPc alone (Table 1, Figure 4C) but still a reduction in J_{SC} compared to the P3HT:$PC_{61}BM$ baseline device. The measured V_{OC} was unchanged, and we observed a more pronounced peak at 610 nm in the EQE spectra when the mixture was used compared to the use of 3MP-BsubPc or F_5-BsubPc alone (Figure 4C). However, the FF was significantly reduced to 37% for the mixture, which is in between the FF of 47% and 33% obtained when using simply 3MP-BsubPc or F_5-BsubPc, respectively.

The sum of these results suggest that, while the BsubPc chromophore has the correct frontier orbital energies to produce a cascade electron transfer between P3HT and $PC_{61}BM$ phases, none of these compounds are as functional as $(3HS)_2$-SiPc. We can conclude then that there is more to consider than having a chromophore with either high or low solubility (take PDP-BsubPc vs F_5-BsubPc, for example) and appropriate frontier orbital energy levels.

During our work with $(3HS)_2$-SiPc, we have observed that it has a unique combination of high solubility and an extraordinarily strong (in our experience) tendency to crystallize. Sasa et al. have reported a single crystal determined structure for $(3HS)_2$-SiPc.[45] In our laboratory, extraordinarily large single crystals of $(3HS)_2$-SiPc were unintentionally grown by leaving the crude $(3HS)_2$-SiPc in a hot pyridine solution and letting it cool to room temperature overnight (Figure 5A). The nonsolvated single crystals were analyzed using X-ray diffraction at a low temperature (CCDC deposition number 988974), and the molecular structure and solid state arrangement of $(3HS)_2$-SiPc was determined with very high accuracy, higher than that reported by Sasa et al.[45] The resulting thermal ellipsoid plot is illustrated in Figure 5B. In spite of the high number of degrees of freedom that would normally be assumed to be associated with a tri-*n*-hexylsilyl group, we found that the crystals of $(3HS)_2$-SiPc have absolutely no disorder in the hexyl chains. Furthermore, the positions of the carbon atoms of the tri-*n*-hexylsilyl groups are well fixed (as indicated by the tight thermal ellipsoids), further indicating a lack of disorder within the crystal. Regarding the solid state arrangement, $(3HS)_2$-SiPc arranges into a well ordered three-dimensional matrix where all the SiPc chromophores are pointing in the same orientation and are separated by interstacking tri-*n*-hexylsilyl groups (Figure 5C,D).

On the basis of the uniqueness of $(3HS)_2$-SiPc seen to this point, we also wanted to determine if the tri-*n*-hexylsilyl groups are essential to the functionality of $(3HS)_2$-SiPc in a BHJ OPV device and its tendency to crystallize. We therefore synthesized an alternative SiPc derivative: bis(3-pentadecyl phenoxy)-silicon phthalocyanine ($(PDP)_2$-SiPc). $(PDP)_2$-SiPc was chosen as target because it is (or was expected to be) a highly soluble SiPc derivative[43] and the 3-pentadecyl phenoxy molecular fragment has a similar number of carbon atoms as the tri-*n*-hexylsilyl oxide group (21 vs 18 carbon atoms). Electrochemical and spectroscopic characterization were performed on $(PDP)_2$-SiPc, and the results are tabulated in Table 2. The respective HOMO and LUMO energy levels (calculated) are similar to those of $(3HS)_2$-SiPc and should therefore also facilitate a cascade electron transfer between the P3HT and $PC_{61}BM$. $(PDP)_2$-SiPc was introduced into a series of P3HT:$PC_{61}BM$ BHJ OPV devices using loadings of 3.7, 5, and 10 wt %. The respective EQE spectra and IV curves for the BHJ OPV devices as well as the corresponding characteristics are illustrated and tabulated in Figure 6 and Table 1, respectively. At low $(PDP)_2$-SiPc loadings (3.7 wt %), a noticeable increase in J_{SC} and consequently the η_{eff} was observed compared to the baseline P3HT:$PC_{61}BM$ OPV (Figure 6, Table 1). Once the loading was increased to 10 wt %, a moderate increase in J_{SC} was observed; however, the significant drop in FF resulted in a drop in η_{eff}. At low loading, this behavior is similar to $(3HS)_2$-SiPc but the similarity deviates at higher loadings.

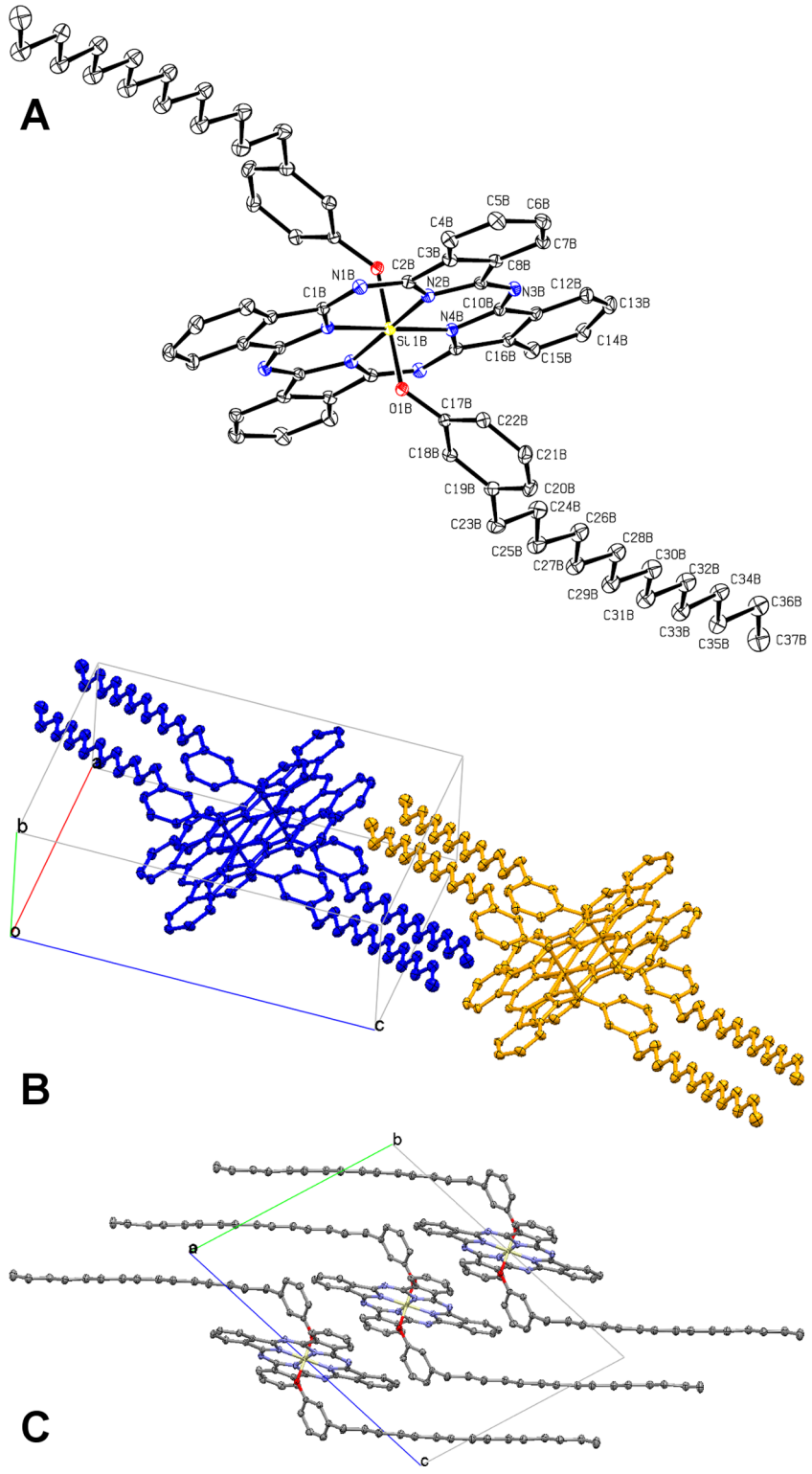

Figure 7. (A) Ellipsoid plot (50% probability) showing the structure and atom number scheme of $(PDP)_2$-SiPc (CCDC deposition number: 988976); (B) and (C) are the solid state arrangement of multiple $(PDP)_2$-SiPc molecules. In (B), each molecule is colored blue or orange for clarity. In all cases, hydrogens are omitted for clarity. The unit cell is shown in (B) and (C).

We also found that $(PDP)_2$-SiPc also has a tendency to crystallize, albeit qualitatively not as strong as $(3HS)_2$-SiPc as indicated by the much smaller crystals obtained. This observation was made despite the expected large degrees of freedom of the 3-pentadecylphenoxy molecular fragments and the high overall solubility of $(PDP)_2$-SiPc. For instance, single crystals of $(PDP)_2$-SiPc could be obtained either by precipitation of a dichloromethane solution into acetonitrile or by simple slow evaporation of a dichloromethane solution. The single crystals of $(PDP)_2$-SiPc that were grown by slow evaporation of a dichloromethane solution were diffracted using X-ray crystallography (CCDC deposition number 988976).

The resulting 50% ellipsoid probability plot is illustrated in Figure 7A. The solid state arrangement of $(PDP)_2$-SiPc is quite different from that of $(3HS)_2$-SiPc (Figure 7B,C), where the SiPc chromophores are closely packed and separated in between the interdigitated pentadecyl molecular fragments (Figure 7B,C).

When comparing the addition of $(3HS)_2$-SiPc versus the addition of $(PDP)_2$-SiPc under similar loadings in a ternary P3HT:$PC_{61}BM$ BHJ OPV device, it is observed that $(3HS)_2$-SiPc is a more effective additive (Table 1, Figure 6). For example, compared to the baseline P3HT:$PC_{61}BM$ BHJ OPV device, the addition of 3.7 wt % of $(3HS)_2$-SiPc resulted in an increase in J_{SC} and η_{eff} of 16% and 20%, respectively, while the addition of 3.7 wt % of $(PDP)_2$-SiPc only resulted in an increase in J_{SC} and η_{eff} of 12% and 10%, respectively. These results indicate that a more significant cascade effect is taking place between P3HT and $PC_{61}BM$ when $(3HS)_2$-SiPc is present. We can offer a possible explanation. We feel the superior performance of $(3HS)_2$-SiPc may be due to its extraordinary tendency to crystallize. Honda et al. has offered plenty of evidence that the majority of the $(3HS)_2$-SiPc resides at the interface between the P3HT and the $PC_{61}BM$ phases.[25−28] We can then hypothesize that the driving force for crystallization is enabling the migration of the $(3HS)_2$-SiPc to the interface. Conversely, $(PDP)_2$-SiPc has a lower tendency to crystallize, so while it does enhance the performance of the BHJ OPV, it does so to a lesser extent; it lacks a strong driving force to migrate to the interface. Considering it in the reverse way, $(PDP)_2$-SiPc could have a higher solubility or affinity for the P3HT phase due hydrocarbon−hydrocarbon interaction between the *n*-hexyl chains of P3HT and the pentadecyl chains of $(PDP)_2$-SiPc resulting in a decreased amount of $(PDP)_2$-SiPc at the P3HT:$PC_{61}BM$ interface compared with $(3HS)_2$-SiPc. Such interactions might not be possible with $(3HS)_2$-SiPc due to the differences in geometry/location of the *n*-hexyl fragments and its own high tendency to crystallize. Another important observation is that a 3.7 or 5.3 wt % loading of $(PDP)_2$-SiPc results in a EQE, at 700 nm, of ≈30%, whereas with a loading of 5.3 wt % of $(3HS)_2$-SiPc the resulting EQE, at 700 nm, is ≈55% (Figures 3 and 6). These observations further suggest that, compared to $(3HS)_2$-SiPc, fewer $(PDP)_2$-SiPc are able to migrate to the P3HT:$PC_{61}BM$ interface and crystallize to participate in the cascade effect, even when increasing the concentration of $(PDP)_2$-SiPc (Figures 3 and 6). We also observed that under higher $(PDP)_2$-SiPc loadings (10.6 wt %) the EQE spectrum consistently demonstrated a second peak at ≈720 nm, which is red-shifted from the peak assigned to the SiPc chromophore (≈700 nm) (Figure 6A). This second peak could be a result of the broadening of the absorption due to the agglomeration of several $(PDP)_2$-SiPc molecules present at high loadings, suggesting the formation of $(PDP)_2$-SiPc clusters. This hypothesis is consistent with the observation reported by Lim et al. whereby the non-*tert*-butylated $(3HS)_2$-SiNc did also form its own crystalline phase which was suppressed to some extent by the incorporation of *tert*-butyl group.[29]

Further supporting this idea that the tendency to crystallize is an important consideration for BHJ OPV additives, we could not obtain crystals of 3HS-BsubPc for X-ray diffraction analysis despite multiple attempts including growth via vapor diffusion (hexanes into DCM or heptanes into benzene), liquid/liquid diffusion by a layering method (DCM to hexanes or benzene to heptane), or slow cooling from hot solvent such as chloroform, dichloromethane, or toluene. Given the lack of tendency to crystallize, 3HS-BsubPc likely stays in either phase and therefore cannot participate in the cascade electron transfer process.

As a final note, we were also able to grow single crystals of $(3HS)_2$-GePc, albeit with significantly more difficulty than for $(3HS)_2$-SiPc. The resulting molecular structure and solid-state arrangement were again analyzed using X-ray diffraction (CCDC deposition number 988975). We found that $(3HS)_2$-GePc has a similar solid state arrangement to that of $(3HS)_2$-SiPc (Figure S13, Supporting Information). However, within this crystal, there was significant disorder observed in the arrangement of one of the three hexyl chains of the tri-*n*-hexylsilyl molecular fragments. The position of the six carbon atoms was distributed between two positions each. The larger ellipsoids generally within all the tri-*n*-hexylsilyl groups also indicate a level of disorder. This is in sharp contrast to what was found (and discussed above) for $(3HS)_2$-SiPc. Given these observations, we can then hypothesize that $(3HS)_2$-GePc does not possess the extraordinary ability to crystallize that $(3HS)_2$-SiPc does. While this does not offer an explanation for the poor BHJ OPV performance seen when $(3HS)_2$-GePc is added to the cell, it does indicate that it is unlikely that $(3HS)_2$-GePc is present at the interface between P3HT and $PC_{61}BM$ rather it is likely solubilized in one or both of the phases.

SUMMARY AND CONCLUSIONS

We have verified the results of Honda et al.[25] that the use of $(3HS)_2$-SiPc as an additive in a ternary P3HT:$PC_{61}BM$:dye BHJ OPV device results in an increase in the J_{SC} and η_{eff} of up to 25% and 20%, respectively. Our original interest was to explore alternatives to $(3HS)_2$-SiPc, and we therefore synthesized similar dyes using different core elements such as germanium and boron and placed the resulting dyes in BHJ OPV devices. We observed that addition of $(3HS)_2$-GePc to the BHJ OPV resulted in a large decrease in cell performance and EQE. We also showed that the presence of 3HS-BsubPc in the BHJ OPV device resulted in a nonstatistical increase in J_{SC} and η_{eff}.

Given the lack of performance of $(3HS)_2$-GePc and 3HS-BsubPc, we further explored the silicon phthalocyanine core. We synthesized a silicon phthalocyanine with solubilizing pentadecyl phenoxy groups ($(PDP)_2$-SiPc, pentadecyl phenoxy having almost equivalent carbon number as tri-*n*-hexylsilyl) and tested the resulting dye in a BHJ OPV device. At low $(PDP)_2$-SiPc loadings (3.7 wt %), J_{SC} and η_{eff} were observed to increase compared to the base P3HT:$PC_{61}BM$ BHJ OPV device; however, when increasing the loading of $(PDP)_2$-SiPc to 5 or 10 wt %, the resulting device η_{eff} dropped below that of the base P3HT:$PC_{61}BM$ BHJ OPV device. Comparing the addition of $(3HS)_2$-SiPc or that of $(PDP)_2$-SiPc, it became clear that $(3HS)_2$-SiPc uniquely resulted in a more significant cascade electron transfer effect manifesting itself in greater increases in J_{SC} and η_{eff}.

The sum of our observations led us to believe that $(3HS)_2$-SiPc is a unique phthalocyanine-based additive to a P3HT:$PC_{61}BM$ BHJ OPV device. Not only does it have appropriate frontier molecular orbital energy levels to facilitate cascade electron transfer but also it is likely that when $(3HS)_2$-SiPc moves to the P3HT:$PC_{61}BM$ interface during deposition (as determined by Honda et al.[28]) it readily crystallizes resulting in better charge transfer between the P3HT and $PC_{61}BM$ phases. We make this assertion based on our observations that despite the high solubility of $(3HS)_2$-SiPc it

also has an extraordinary tendency to crystallize. It is possible that the driving force for crystallization of $(3HS)_2$-SiPc is the reason it moves to a large extent to the P3HT/$PC_{61}BM$ interface. Conversely, the reason 3HS-BsubPc and $(PDP)_2$-SiPc are not as effective as $(3HS)_2$-SiPc despite having appropriate frontier orbitals is because they do not crystallize as easily, in other words, there is a limited driving force for them to crystallize and thus a significant portion remains outside of the interface between P3HT and $PC_{61}BM$. These findings represent a possible explanation as to why $(3HS)_2$-SiPc is such a good dye in assisting P3HT:$PC_{61}BM$ BHJ OPV devices and that the choice of the tri-*n*-hexylsilyl substituent is crucial to its performance. Tri-*n*-hexylsilyl substituents offer the necessary solubilizing properties while offering ease for crystallization for a silicon phthalocyanine when in the solid state, resulting in favorable dispersion and charge transfer between the P3HT and the $PC_{61}BM$.

EXPERIMENTAL SECTION

Materials. All ACS grade solvents were purchased from Caledon Laboratories (Caledon, Ontario, Canada) and used without further purification unless otherwise stated. Tri-*n*-hexylchlorosilane was purchased from Gelest (Morrisville, Pennsylvania, USA) and used as received. Deuterated chloroform ($CDCl_3$) with 0.05% (v/v) tetramethylsilane (TMS) was purchased from Cambridge Isotope Laboratories, Inc. (St. Leonard, Quebec, Canada) and used as received. Thin layer chromatography (TLC) was performed on aluminum plates coated with silica (pore size of 60 Å) and fluorescent indicator, obtained from Whatman Ltd., and visualized under UV (254 nm) light. Column chromatography was performed using Silica Gel P60 (mesh size 40−63 μm) obtained from SiliCycle Inc. (Quebec City, Quebec, Canada). Hydroxy-boron subphthalocyanine (HO-BsubPc),[46] dichloro silicon phthalocyanine ($(Cl)_2$-SiPc),[47] dichloro germanium phthalocyanine ($(Cl)_2$-GePc),[48] 3-pentadecylphenoxy boron subphthalocyanine (PDP-BsubPc),[43] 3-methylphenoxy boron subphthalocyanine (3MP-BsubPc),[44] and pentafluorophenoxy boron subphthalocyanine (F_5-BsubPc)[49] were all prepared according to the literature.

Methods. All reactions were performed under an atmosphere of argon gas using oven-dried glassware. Nuclear magnetic resonance (NMR) spectra were recorded on a Bruker Avance III spectrometer at 23 °C in $CDCl_3$, operating at 400 MHz for ^{1}H NMR and 100 MHz for ^{13}C NMR. Chemical shifts (δ) are reported in parts per million (ppm) referenced to tetramethylsilane (0 ppm) for ^{1}H NMR and $CDCl_3$ (77.16 ppm) for ^{13}C NMR. Coupling constants (J) are reported in hertz (Hz). Spin multiplicities are designated by the following abbreviations: s (singlet), d (doublet), t (triplet), q (quartet), m (multiplet), and br (broad). Accurate mass determinations (HRMS) were carried out on a GCT Premier TOF mass spectrometer (Waters Corporation, Milford, Massachusetts, USA). Low resolution mass spectroscopy (LRMS) was acquired on a AccuTOF model JMS-T1000LC mass spectrometer (JEOL USA Inc., Peabody, Massachusetts, USA) equipped with a Direct Analysis in Real Time (DART) ion source or on a GC Premier TOF mass spectrometer (Waters Corporation, Milford, Massachusetts, USA) with EI/CI sources. Ultraviolet−visible (UV−vis) absorption spectra were acquired on a PerkinElmer Lambda 1050 UV/vis/NIR spectrometer using a PerkinElmer quartz cuvette with a 10 mm path length. Photoluminescence (PL) spectra were recorded on a PerkinElmer LS55 fluorescence spectrometer using a PerkinElmer quartz cuvette with a 10 mm path length. High pressure liquid chromatography (HPLC) analysis was carried out on a Waters 2695 separation module with a Waters 2998 photodiode array and a Waters Styragel HR 2 THF 4.6 × 300 mm column. The mobile phase used was HPLC grade acetonitrile (80% by volume) and *N,N*-dimethylformamide (20% by volume). Cyclic voltammetry was carried out using a Bioanalytical Systems C3 electrochemical workstation. The working electrode was a 2 mm glassy carbon disk; the counter electrode was a platinum wire, and the reference electrode was $Ag/AgCl_2$ saturated salt solution. Spec-grade dichloromethane was purged with nitrogen gas at room temperature prior to its use. Three cycles from +1.7 to −1.7 V at a scan rate of 100 mV/s were measured for each sample. Tetrabutylammonium perchlorate (1 M) was used as the supporting electrolyte, and decamethylferrocene was used as an internal reference.

Synthetic Procedures. *Tri-n-hexylsiloxy-boron Subphthalocyanine (3HS-BsubPc).* To an oven-dried three-neck round-bottom flask was added HO-BsubPc (0.50 g, 1.21 mmol, 1 equiv), 1,2-dichlorobenzene (20 mL), and tri-*n*-hexylchlorosilane (0.90 mL, 2.46 mmol, 2 equiv) under argon. The reaction mixture was heated to 130 °C, and the reaction was monitored by HPLC (acetonitrile/*N,N*-dimethylformamide, 80:20 v/v) for the consumption of HO-BsubPc. Once the reaction had stopped progressing (~5 h), the reaction mixture was cooled to room temperature before it was concentrated under reduced pressure to a dark pink liquid. Note that further addition of tri-*n*-hexylchlorosilane to the reaction mixture did not consume any unreacted HO-BsubPc. The crude product was purified via silica gel column chromotography using 100% hexane to first elute unreacted tri-*n*-hexylchlorosilane and other silane derivatives, followed by a gradient to 20% THF solution in hexane (v/v) to elute the target compound as a bright pink solid (yield = 49%) following rotary evaporation. ^{1}H NMR (400 MHz, $CDCl_3$) δ 8.87−8.81 (m, 6H), 7.92−7.85 (m, 6H), 1.14−1.04 (m, 6H), 0.96−0.89 (m, 6H), 0.89−0.81 (m, 6H), 0.78 (t, J = 7.3 Hz, 9H), 0.51−0.42 (m, 6H), −0.38−0.45 (m, 6H); ^{13}C NMR (100 MHz, $CDCl_3$) δ 151.0, 131.2, 129.6, 122.2, 33.2, 31.6, 22.9, 22.7, 14.5, 14.3; HRMS (EI) [M] calcd for 694.3987, found 694.3990.

Bis(hydroxy)-silicon Phthalocyanine ($(HO)_2$-SiPc). To an oven-dried three-neck round-bottom flask was added Cl_2-SiPc (2.5 g, 4.09 mmol, 1 equiv), 1,2-dichlorobenzene (25 mL), and cesium hydroxide (1.50 g, 10.0 mmol, 2.5 equiv) under argon. The reaction mixture was heated to 120 °C for 4 h. The crude product was precipitated into methanol and filtered to give a dark blue powder (crude yield = 54%), which was used without further purification. LRMS (EI) calcd for 574.62, found 574.1.

Bis(hydroxy)-germanium Phthalocyanine ($(HO)_2$-GePc). $(HO)_2$-GePc was synthesized using the same method as $(HO)_2$-SiPc. The crude product was precipitated into methanol and filtered to give a dark blue solid (crude yield = 78%), which was used without further purification. Mass spectrometry data could not be obtained as fragmentation of the title compound occurs.

Bis(tri-n-hexylsiloxy)-silicon Phthalocyanine ($(3HS)_2$-SiPc). $(3HS)_2$-SiPc was synthesized from $(HO)_2$-SiPc by adapting the patent literature.[30] To an oven-dried three-neck round-bottom flask was added $(HO)_2$-SiPc (1.00 g, 1.61 mmol, 1 equiv), pyridine (100 mL), and tri-*n*-hexylchlorosilane (4.85 g, 17.1 mmol, 5 equiv per reactive site) under argon. The reaction mixture was heated to 130 °C for 5 h before it was cooled to room temperature. The crude product was precipitated into water, filtered, washed with water (3×), and dried in a vacuum oven to give a dark blue solid (yield = 79% before column chromatography, purity >90% as determined by ^{1}H NMR). The crude product was purified via silica gel column chromatography using 100% hexane to first elute unreacted tri-*n*-hexylchlorosilane and other silane derivatives, followed by a gradient to 50% THF solution in hexane (v/v) to elute the target compound as a dark blue solid (yield = 47%) following rotary evaporation. Single crystals of $(3HS)_2$-SiPc were grown by slow cooling from hot pyridine solution. ^{1}H NMR (400 MHz, $CDCl_3$) δ 9.66−9.60 (m, 8H), 8.33−8.28(m, 8H), 0.87−0.79 (m, 12H), 0.74−0.67 (t, J = 7.2 Hz, 18H), 0.62−0.55 (m, 12H), 0.40−0.32 (m, 12H), 0.06−0.03 (m, 12H), −1.21−1.35 (m, 12H); ^{13}C NMR (100 MHz, $CDCl_3$) δ 148.9, 136.4, 130.6, 123.6, 33.6, 33.4, 32.8, 31.8, 31.7, 31.1, 23.4, 23.2, 22.80, 22.75, 22.6, 21.5, 16.0, 15.2, 14.31, 14.29, 14.27, 12.9; LRMS (EI) m/z $[M + H]^+$calcd for 1139.78, found 1139.7.

Bis(tri-n-hexylsiloxy)-germanium Phthalocyanine ($(3HS)_2$-GePc). $(3HS)_2$-GePc was synthesized from $(OH)_2$-GePc in an identical fashion to that of $(3HS)_2$-SiPc. The title compound was obtained as a dark blue solid (yield = 49%). Single crystals of $(3HS)_2$-GePc were grown by slow cooling from DCM/hexanes. ^{1}H NMR (400 MHz,

$CDCl_3$) δ 9.66−9.61 (m, 8H), 8.34−8.29 (m, 8H), 0.86−0.78 (m, 12H), 0.73−0.68 (m, 18H), 0.62−0.55 (m, 12H), 0.41−0.32 (m, 12H), 0.06−0.02 (m, 12H), −1.07−1.17 (m, 12H); ^{13}C NMR (100 MHz, $CDCl_3$) δ 149.6, 135.9, 131.5, 124.1, 33.4, 32.7, 31.7, 31.1, 29.92, 29.87, 23.2, 22.8, 22.5, 21.7, 15.2, 14.3, 14.3, 13.4. Mass spectrometry data could not be obtained as fragmentation of the title compound occurs.

Bis(3-pentadecylphenoxy)-silicon Phthalocyanine ($(PDP)_2$-SiPc). In a procedure adapted from Brisson et al.,[40] Cl_2-SiPc (0.5 g, 0.82 mmol, 1 equiv) and 3-pentadecylphenol (0.60 g, 1.97 mmol, 2.4 equiv) were added to chlorobenzene (30 mL) under argon and heated to 120 °C for 22 h. Upon cooling to room temperature, the reaction mixture was concentrated to dryness via rotary evaporation. Some of the 3-pentadecylphenol was removed via distillation at 200 °C using a rotary evaporator equipped with a high vacuum pump. The resulting dark blue solid was eluted on a silica gel column using DCM as the eluent. The first eluted blue band was collected, concentrated, and dried in a vacuum oven to give a dark blue solid (yield = 38%). Single crystals of $(PDP)_2$-SiPc were grown by slow evaporation from dichloromethane solution. ^{1}H NMR (400 MHz, $CDCl_3$) 9.68−9.61 (m, 8H), 8.38−8.30 (m, 8H), 5.55−5.51 (m, 2H), 5.51−5.46 (t, J = 7.5 Hz, 2H), 2.34−2.29 (m, 2H), 2.26−2.23 (m, 2H), 1.39−1.26 (m, 40H), 1.25−1.16 (m, 4H), 1.14−1.04 (m, 4H), 0.96−0.90 (m, 6H), 0.85−0.75 (m, 4H), 0.61−0.50 (m, 4H); ^{13}C NMR (100 MHz, $CDCl_3$) δ 149.8, 149.3, 142.1, 135.9, 131.1, 126.6, 123.9, 119.5, 117.5, 114.8, 34.8, 32.1, 30.5, 30.0, 29.94, 29.88, 29.8, 29.6, 29.5, 29.3, 22.9, 14.3; HRMS (DART) m/z $[M + H]^+$ calcd for 1147.61, found 1147.6.

Device Fabrication and Testing. P3HT:PC_{61}BM:dye containing devices were made by dissolving the P3HT, PC_{61}BM, and the dye in 1,2-dichlorobenzene (40 mg/mL solutions) and were allowed to stirred at 50 °C for 2−3 h to ensure complete dissolution of the solids. Indium tin oxide (ITO) coated glass substrates (Colorado Concept Coatings LLC) were rubbed with aqueous detergent followed by ultrasonication in aqueous detergent, deionized water, acetone, and methanol for 5 min each, followed by an oxygen-plasma treatment for 15 min. A thin layer of poly(3,4-ethylenedioxythiophene):poly(styrene sulfonic acid) (PEDOT:PSS) was then spin-coated onto the ITO glass at 3000 rpm for 30 s and dried in air at 140 °C on a hot plate for 15 min. Prior to spin coating the active layer, the P3HT, the PC_{61}BM, and the dye solutions were stirred together for 15 min. The ternary mixtures were then spin-coated onto the PEDOT:PSS coated substrates at 600 rpm under nitrogen atmosphere and allowed to dry at room temperature for 20 h. No annealing was performed on these devices. The substrates were then coated with lithium fluoride (LiF, 0.8 nm) and aluminum (Al, 100 nm) by thermal evaporation using an Angstrom Engineering (Kitchener, ON) Covap II metal evaporation system at 0.7−2.0 × 10^{-6} Torr. The device area is 0.07 cm^2 as defined by a shadow mask, and the IV curves were obtained using a Keithley 2400 source meter under simulated AM 1.5G conditions. The the spectrum mismatch was calibrated using a Si diode with a KG-5 filter. EQE measurements were recorded using a 300 W xenon lamp with an Oriel Cornerstone 260 1/4 m monochromator and compared with a Si reference device that is traceable to the National Institute of Standards and Technology.

■ ASSOCIATED CONTENT

Ⓢ Supporting Information

^{1}H NMR and ^{13}C NMR spectroscopy, mass spectrometry spectra of various novel compounds, and a discussion on the effect of loading BsubPc and its effect on the photogeneration of BHJ. This material is available free of charge via the Internet at http://pubs.acs.org/.

■ AUTHOR INFORMATION

Corresponding Author

*Tel: 1-416-978-6140. E-mail: tim.bender@utoronto.ca.

Notes

The authors declare no competing financial interest.

■ ACKNOWLEDGMENTS

The authors would like to acknowledge financial support from Saudi Basic Industries (SABIC). We would like to acknowledge the Natural Sciences and Engineering Research Council (NSERC) of Canada for their support through the Discovery Grant program. B.H.L. would like to thank the government of Canada for the Banting Post-Doctoral Fellowship. The authors also acknowledge Dr. Alan Lough (Department of Chemistry, University of Toronto) for performing the single crystal X-ray analyses.

■ REFERENCES

(1) Nayak, P.; Bisquert, J.; Cahen, D. Assessing Possibilities and Limits for Solar Cells. *Adv. Mater.* **2011**, *23*, 2870−2876.
(2) Brunetti, F.; Kumar, R.; Wudl, F. Organic Electronics From Perylene to Organic Photovoltaics: Painting a Brief History with a Broad Brush. *J. Mater. Chem.* **2010**, *20*, 2934−2948.
(3) Dennler, G.; Scharber, M.; Brabec, C. J. Polymer-Fullerene Bulk-Heterojunction Solar Cells. *Adv. Mater.* **2009**, *21*, 1323−1338.
(4) Cai, W.; Gong, X.; Cao, Y. Polymer Solar Cells: Recent Development and Possible Routes for Improvement in the Performance. *Sol. Energy Mater. Sol. Cells* **2010**, *94*, 114−127.
(5) Wang, D. H.; Moon, J. S.; Seifter, J.; Jo, J.; Park, J. H.; Park, O. O.; Heeger, A. J. Sequential Processing: Control of Nanomorphology in Bulk Heterojunction Solar Cells. *Nano Lett.* **2011**, *11*, 3163−3168.
(6) Moon, J. S.; Takacs, C. J.; Sun, Y.; Heeger, A. J. Spontaneous Formation of Bulk Heterojunction Nanostructures: Multiple Routes to Equivalent Morphologies. *Nano Lett.* **2011**, *11*, 1036−1039.
(7) Ayzner, A. L.; Tassone, C. J.; Tolbert, S. H.; Schwartz, B. J. Reappraising the Need for Bulk Heterojunctions in Polymer−Fullerene Photovoltaics: The Role of Carrier Transport in All-Solution-Processed P3HT/PCBM Bilayer Solar Cells. *J. Phys. Chem. C* **2009**, *113*, 20050−20060.
(8) Morse, G. E.; Gantz, J. L.; Steirer, K. X.; Armstrong, N. R.; Bender, T. P. Pentafluorophenoxy Boron Subphthalocyanine (F5BsubPc) as a Multifunctional Material for Organic Photovoltaics. *ACS Appl. Mater. Interfaces* **2013**, *6*, 1515−1524.
(9) He, Z.; Zhong, C.; Huang, X.; Wong, W.-Y.; Wu, H.; Chen, L.; Su, S.; Cao, Y. Simultaneous Enhancement of Open-Circuit Voltage, Short-Circuit Current Density, and Fill Factor in Polymer Solar Cells. *Adv. Mater.* **2011**, *23*, 4636−4643.
(10) Chen, H.-Y.; Hou, J.; Zhang, S.; Liang, Y.; Yang, G.; Yang, Y.; Yu, L.; Wu, Y.; Li, G. Polymer Solar Cells with Enhanced Open-Circuit Voltage and Efficiency. *Nat. Photonics* **2009**, *3*, 649−653.
(11) Zhou, H.; Yang, L.; Stuart, A. C.; Price, S. C.; Liu, S.; You, W. Development of Fluorinated Benzothiadiazole as a Structural Unit for a Polymer Solar Cell of 7% Efficiency. *Angew. Chem., Int. Ed.* **2011**, *50*, 2995−2998.
(12) Service, R. F. Outlook Brightens for Plastic Solar Cells. *Science* **2011**, *332*, 293.
(13) Guo, X.; Zhou, N.; Lou, S. J.; Smith, J.; Tice, D. B.; Hennek, J. W.; Ortiz, R. P.; Navarrete, J. T. L.; Li, S.; Strzalka, J.; Chen, L. X.; Chang, R. P. H.; Facchetti, A.; Marks, T. J. Polymer Solar Cells with Enhanced Fill Factors. *Nat. Photonics* **2013**, *7*, 825−833.
(14) Dang, M. T.; Hirsch, L.; Wantz, G. P3HT:PCBM, Best Seller in Polymer Photovoltaic Research. *Adv. Mater.* **2011**, *23*, 3597−3602.
(15) Dang, M. T.; Hirsch, L.; Wantz, G.; Wuest, J. D. Controlling the Morphology and Performance of Bulk Heterojunctions in Solar Cells. Lessons Learned From the Benchmark Poly(3-Hexylthiophene):[6,6]-Phenyl-C 61-Butyric Acid Methyl Ester System. *Chem. Rev.* **2013**, *113*, 3734−3765.
(16) Blouin, N.; Michaud, A.; Gendron, D.; Wakim, S.; Blair, E.; Neagu-Plesu, R.; Belletête, M.; Durocher, G.; Tao, Y.; Leclerc, M. Toward a Rational Design of Poly(2,7-Carbazole) Derivatives for Solar Cells. *J. Am. Chem. Soc.* **2008**, *130*, 732−742.

(17) Boudreault, P.-L. T.; Najari, A.; Leclerc, M. Processable Low-Bandgap Polymers for Photovoltaic Applications. *Chem. Mater.* **2011**, *23*, 456−469.
(18) Chen, Y.-C.; Hsu, C.-Y.; Lin, R. Y.-Y.; Ho, K.-C.; Lin, J. T. Materials for the Active Layer of Organic Photovoltaics: Ternary Solar Cell Approach. *ChemSusChem* **2013**, *6*, 20−35.
(19) Khlyabich, P. P.; Burkhart, B.; Thompson, B. C. Compositional Dependence of the Open-Circuit Voltage in Ternary Blend Bulk Heterojunction Solar Cells Based on Two Donor Polymers. *J. Am. Chem. Soc.* **2012**, *134*, 9074−9077.
(20) Khlyabich, P. P.; Burkhart, B.; Thompson, B. C. Efficient Ternary Blend Bulk Heterojunction Solar Cells with Tunable Open-Circuit Voltage. *J. Am. Chem. Soc.* **2011**, *133*, 14534−14537.
(21) Kozycz, L. M.; Gao, D.; Hollinger, J.; Seferos, D. S. Donor-Donor Block Copolymers for Ternary Organic Solar Cells. *Macromolecules* **2012**, *45*, 5823−5832.
(22) Ameri, T.; Khoram, P.; Min, J.; Brabec, C. J. Organic Ternary Solar Cells: A Review. *Adv. Mater.* **2013**, *25*, 4245−4266.
(23) Ye, L.; Xia, H.; Xiao, Y.; Xu, J.; Miao, Q. Ternary Blend Bulk Heterojunction Photovoltaic Cells with an Ambipolar Small Molecule as the Cascade Material. *RSC Adv.* **2014**, *4*, 1087−1092.
(24) Chen, M. C.; Liaw, D. J.; Huang, Y. C.; Wu, H. Y.; Tai, Y. Improving the Efficiency of Organic Solar Cell with a Novel Ambipolar Polymer to Form Ternary Cascade Structure. *Sol. Energy Mater. Sol. Cells* **2011**, *95*, 2621−2627.
(25) Honda, S.; Nogami, T.; Ohkita, H.; Benten, H.; Ito, S. Improvement of the Light-Harvesting Efficiency in Polymer/Fullerene Bulk Heterojunction Solar Cells by Interfacial Dye Modification. *ACS Appl. Mater. Interfaces* **2009**, *1*, 804−810.
(26) Honda, S.; Ohkita, H.; Benten, H.; Ito, S. Multi-Colored Dye Sensitization of Polymer/Fullerene Bulk Heterojunction Solar Cells. *Chem. Commun.* **2010**, *46*, 6596−6598.
(27) Honda, S.; Ohkita, H.; Benten, H.; Ito, S. Selective Dye Loading at the Heterojunction in Polymer/Fullerene Solar Cells. *Adv. Energy Mater.* **2011**, *1*, 588−598.
(28) Honda, S.; Yokoya, S.; Ohkita, H.; Benten, H.; Ito, S. Light-Harvesting Mechanism in Polymer/Fullerene/Dye Ternary Blends Studied by Transient Absorption Spectroscopy. *J. Phys. Chem. C* **2011**, *115*, 11306−11317.
(29) Lim, B.; Bloking, J. T.; Ponec, A.; McGehee, M. D.; Sellinger, A. Ternary Bulk Heterojunction Solar Cells: Addition of Soluble NIR Dyes for Photocurrent Generation beyond 800 nm. *ACS Appl. Mater. Interfaces* **2014**, *6*, 6905−6913.
(30) Gessner, T.; Sens, R.; Ahlers, W. Preparation of Silicon Phthalocyanines and Germanium Phthalocyanines and Related Substances. U.S. Patent US 2010/0113767 A1, May 6, 2010.
(31) Meyer, G.; Wöhrle, D. Dark Conductivities of Low Molecular and Polymer Phthalocyanines Containing IVa-Group Elements. *Mater. Sci.-Polym.* **1981**, *7*, 265−270.
(32) Branston, R.; Duff, J.; Hsiao, C. K.; Loutfy, R. O. Photovoltaic Properties of Organic Photoactive Particle Dispersions: Polymeric Phthaloycanines. In *Polymers in Solar Energy Utilization*; Gebelein, C. G., Williams, D. J., Deanin, R. D., Eds.; ACS Symposium Series; American Chemical Society: Washington, D. C., 1983; Vol. *220*, pp 437−455.
(33) Morse, G. E.; Bender, T. P. Boronsubphthalocyanines as Organic Electronic Materials. *ACS Appl. Mater. Interfaces* **2012**, *4*, 5055−5068.
(34) Helander, M. G.; Morse, G. E.; Qiu, J.; Castrucci, J. S.; Bender, T. P.; Lu, Z.-H. Pentafluorophenoxy Boron Subphthalocyanine as a Fluorescent Dopant Emitter in Organic Light Emitting Diodes. *ACS Appl. Mater. Interfaces* **2010**, *2*, 3147−3152.
(35) Mauldin, C. E.; Piliego, C.; Poulsen, D.; Unruh, D. A.; Woo, C.; Ma, B.; Mynar, J. L.; Fréchet, J. M. J. Axial Thiophene−Boron-(Subphthalocyanine) Dyads and Their Application in Organic Photovoltaics. *ACS Appl. Mater. Interfaces* **2010**, *2*, 2833−2838.
(36) Ma, B.; Woo, C. H.; Miyamoto, Y.; Fréchet, J. M. J. Solution Processing of a Small Molecule, Subnaphthalocyanine, for Efficient Organic Photovoltaic Cells. *Chem. Mater.* **2009**, *21*, 1413−1417.
(37) Ma, B.; Miyamoto, Y.; Woo, C. H.; Fréchet, J. M. J.; Zhang, F.; Liu, Y. Solution Processable Boron Subphthalocyanine Derivatives as Active Materials for Organic Photovoltaics. In *Organic Photovoltaics X*; Kafafi, Z. H., Lane, P. A., Eds.; SPIE Proceedings; Society of Photo-Optical Instrumentation Engineers: Bellingham, W.A., 2009; Vol. *7416*, pp E-1−E-6.
(38) Cho, S. W.; Piper, L. F. J.; DeMasi, A.; Preston, A. R. H.; Smith, K. E.; Chauhan, K. V.; Sullivan, P.; Hatton, R. A.; Jones, T. S. Electronic Structure of C 60/Phthalocyanine/ITO Interfaces Studied Using Soft X-ray Spectroscopies. *J. Phys. Chem. C* **2010**, *114*, 1928−1933.
(39) Beaumont, N.; Cho, S. W.; Sullivan, P.; Newby, D.; Smith, K. E.; Jones, T. S. Boron Subphthalocyanine Chloride as an Electron Acceptor for High-Voltage Fullerene-Free Organic Photovoltaics. *Adv. Funct. Mater.* **2011**, *22*, 561−566.
(40) Pandey, R.; Zou, Y.; Holmes, R. J. Efficient, Bulk Heterojunction Organic Photovoltaic Cells Based on Boron Subphthalocyanine Chloride-C70. *Appl. Phys. Lett.* **2012**, *101*, 033308-1−033308-4.
(41) Renshaw, C. K.; Xu, X.; Forrest, S. R. A Monolithically Integrated Organic Photodetector and Thin Film Transistor. *Org. Electron.* **2010**, *11*, 175−178.
(42) Yasuda, T.; Tsutsui, T. N-Channel Organic Field-Effect Transistors Based on Boron-Subphthalocyanine. *Mol. Cryst. Liq. Cryst.* **2006**, *462*, 3−9.
(43) Brisson, E. R. L.; Paton, A. S.; Morse, G. E.; Bender, T. P. Boron Subphthalocyanine Dyes: 3-Pentadecylphenol as a Solubilizing Molecular Fragment. *Ind. Eng. Chem. Res.* **2011**, *50*, 10910−10917.
(44) Paton, A. S.; Lough, A. J.; Bender, T. P. One Well-Placed Methyl Group Increases the Solubility of Phenoxy Boronsubphthalocyanine Two Orders of Magnitude. *Ind. Eng. Chem. Res.* **2012**, *51*, 6290−6296.
(45) Sasa, N.; Okada, K.; Nakamura, K.; Okada, S. Synthesis, Structural and Conformational Analysis and Chemical Properties of Phthalocyaninatometal Complexes. *J. Mol. Struct.* **1998**, *446*, 163−178.
(46) Fulford, M. V.; Lough, A. J.; Bender, T. P. The First Report of the Crystal Structure of Non-Solvated M-Oxo Boron Subphthalocyanine and the Crystal Structures of Two Solvated Forms. *Acta Crystallogr., Sect. B: Struct. Sci.* **2012**, *68*, 636−645.
(47) Lowery, M. K.; Starshak, A. J.; Esposito, J. N.; Krueger, P. C.; Kenney, M. E. Dichloro(phthalocyanino)silicon. *Inorg. Chem.* **1965**, *4*, 128.
(48) Joyner, R. D.; Kenney, M. E. Germanium Phthalocyanines. *J. Am. Chem. Soc.* **1960**, *82*, 5790−5791.
(49) Morse, G. E.; Helander, M. G.; Maka, J. F.; Lu, Z.-H.; Bender, T. P. Fluorinated Phenoxy Boron Subphthalocyanines in Organic Light-Emitting Diodes. *ACS Appl. Mater. Interfaces* **2010**, *2*, 1934−1944.
(50) Noviandri, I.; Brown, K. N.; Fleming, D. S.; et al. The Decamethylferrocenium/Decamethylferrocene Redox Couple: A Superior Redox Standard to the Ferrocenium/Ferrocene Redox Couple for Studying Solvent Effects on the Thermodynamics of Electron Transfer. *J. Phys. Chem. B* **1999**, *103*, 6713−6722.
(51) Li, Y.; Cao, Y.; Gao, J.; Wang, D.; Yu, G.; Heeger, A. J. Electrochemical Properties of Luminescent Polymers and Polymer Light-Emitting Electrochemical Cells. *Synth. Met.* **1999**, *99*, 243−248.
(52) Li, S.; Yuan, Z.; Yuan, J.; Deng, P.; Zhang, Q.; Sun, B. An Expanded Isoindigo Unit as a New Building Block for a Conjugated Polymer Leading to High-Performance Solar Cells. *J. Mater. Chem. A* **2014**, *2*, 5427−5433.